Structural Durability & Health Monitoring
DOI:10.32604/sdhm.2020.08221
Article

Mechanical Experimental Study on Tensile Bolted Connections of Cross-laminated Timber

Chenxiao Su and Haibei Xiong*

Department of Disaster Mitigation for Structures, Tongji University, Shanghai, 200092, China
*Corresponding Author: Haibei Xiong. Email: xionghaibei@tongji.edu.cn
Received: 07 August 2019; Accepted: 30 October 2019

Abstract: In order to explore a kind of high-strength, earthquake-resistant, economical and suitable connection, 4 groups of cross-laminated timber wall-to-floor and wall-to-wall bolted connections were tested under monotonic and cyclic loading. The deformation characteristics and failure modes of the cross-laminated timber wall-to-floor and wall-to-wall bolted connections were exploited. Load-slip curves, bearing capacity, yielding point, stiffness and ductility of each group of specimens were analyzed. The test results indicate that the loading process of cross-laminated timber bolted connections under tension can be categorized as five stages, namely the elastic stage, the slip stage, the embedding stage, the yielding stage and the ultimate stage. The ultimate tensile capacity of cross-laminated timber bolted wall-to-floor connections is 2.67 times that of the wall-to-wall bolted connections. Compared with cross-laminated timber self-tapping screwed connections, the ultimate tensile capacity of the cross-laminated timber wall-to-floor bolted connections is 2.70 times that of the self-tapping screwed connections, and the ultimate tensile capacity of the cross-laminated timber wall-to-wall bolted connections is 3.83 times that of the self-tapping screwed connections. The cross-laminated timber bolted connections have larger yielding displacement and wider plastic range, and they are more energy dissipative and more ductile. Furthermore, the cost of the cross-laminated timber wall-to-floor bolted connections is 46% that of the self-tapping screwed connections, while the cost of cross-laminated wall-to-wall bolted connections is 53% that of the self-screwed connections.

Keywords: Cross-laminated timber; bolted connections; mechanical properties; economical and suitable

1 Introduction

Cross-laminated Timber (abbreviated as CLT or X-lam) is a kind of innovative engineered wood product used for construction material. CLT buildings gain superior advantages over the other types of building such as concrete or masonry buildings in the following aspects: higher ratio of strength to weight, good structural integrity, convenience in modularization and prefabrication, good seismic performance. Thus CLT has become a hot topic in timber building research in recent years.

The connections in CLT buildings serve as an important function of joining CLT components to form an integrity and transferring loads. The connections in CLT buildings are mainly composed of wall-to-floor connections, wall-to-wall connections, wall-to-roof connections and wall-to-foundation connections. Wall-to-floor connections are mainly designed to resist the uplift force caused by the overturning moment under horizontal actions such as wind load and earthquake. Wall-to-wall connections are designed to minimize the relative slip between adjacent wall panels and help to keep the integrity of the box-like structure of CLT buildings. Furthermore, since the CLT panels have high in-plane stiffness relative to the connectors, a major portion of the energy dissipative capacity is provided by the metal connections, while the CLT wall panels remain in the elastic domain [1].

The mainstreamed connectors for CLT connections at present are screws, hold-downs, and angle brackets. Muñoz et al. [2] conducted an exploratory study focused on the evaluation of connection performance in European CLT product using normal wood screws and self-tapping screws. Flatscher et al. [3] gave a brief overview of the results obtained from experimental monotonic and cyclic tests that were carried out not only on screwed CLT single joints, but also on wall tests with screwed joints. Gavric et al. [4] performed in-plane monotonic and cyclic shear and withdrawal tests on screwed wall-to-wall and wall-to-floor CLT connections. Mechanical properties such as strength, stiffness, energy dissipation, ductility ratio and impairment of strength were evaluated. Gavric et al. [5] also conducted monotonic and cyclic tests in shear and tension (pull-out) on hold-downs and steel angle brackets used to anchor the wall panels to foundations or to connect wall panels to floor panels. The tests results showed that significant ductility and energy dissipation was attained in most of the tests. Nevertheless, brittle failure modes were observed in some tests. Tomasi [6] carried out a total amount of 115 tests on different configurations of angle brackets elements (77 monotonic tests and 38 cyclic tests), taking into account of the possibility of different fastener types and assembly configurations. The influence on the mechanical properties of the angle bracket geometry and of the number of steel anchors (single or double) was compared. Izzi et al. [7] investigated the mechanical and the hysteretic behaviour of steel-to-timber joints with annular-ringed shank nails in CLT. Average and characteristic values of the experimental strength capacities were evaluated and compared to the analytical predictions determined according to current structural design codes and literature. Furthermore, the overstrength factor and the strength degradation factor are evaluated and conservative values are recommended. Yin-Lan et al. [8] used a series of connection tests and CLT shear walls tests subjected to general quasi-static monotonic and cyclic loading protocols undertaken at FPInnovations of Canada to calibrate two hysteretic models (Saws model and Pinching4 model) in OpenSees. The wall modelling results based on three types of connections are compared with the corresponding full scale CLT wall tests results. Cao et al. [9] investigated the mechanical properties of three types of CLT connections: an angle bracket joint; a crossed self-tapping screw joint; and a simple butt joint with self-tapping screws. Three repetition tests for each type of CLT connection were conducted under two different cyclic-loading protocols. The experimental results showed that pull-out failure in the tension direction was dominant, whereas wood crushing and screw failure were typical failure modes in the shear direction. Apart from traditional connectors for CLT connections, innovative connectors have been rising up during recent years. Latour et al. [10] introduced dissipative connectors called XL-stub in order to improve the seismic performance of CLT panel buildings in substitution of the classical hold-downs because hold-downs exhibit a limited dissipation capacity demonstrated by past experimental tests and numerical analyses. Besides, a newly designed connection system called X-RAD is highlighted in Italy. This innovative connector X-RAD consists of a point-to-point mechanical connection system, fixed to the corners of the CLT panels [11]. This connection, designed to be prefabricated, comprises a metal wrapping and an inner hard wood element which are fastened to the panel by means of full-threaded self-tapping screws [12,13]. Specimens connected with X-RAD were tested in tension and shear under monotonic and cyclic loading protocols, and the test results showed that X-RAD had both high strength, stiffness and good energy dissipative capacity, which were necessary properties appropriate for earthquake-prone areas.

Although extensive research with regard to CLT wall-to-floor and wall-to-wall connections has been carried out, few studies about the application of bolted connections in CLT are mentioned. Bolted connections are now widely applicable to common timber structures, and a wide range of correlated research has been conducted. Ringhofer et al. [14] reviewed approaches for calculating characteristic values as provided in literature for single dowel-type fasteners and connections in CLT. These approaches were compared with the current regulations on dowel-type fasteners and connections for solid timber and glulam as formulated in Eurocode 5 with focus on withdrawal and embedment strength of dowels, nails and self-tapping screws. Conclusions were drawn in respect of the single fastener properties withdrawal and embedment strength and suggest some execution guidelines, which ensured the integrity of CLT structures. Uibel et al. [15] discussed the results of embedment tests, withdrawal tests and connection tests and gave proposals for the calculation of characteristic values. On this basis calculation models for the load carrying capacity of joints with dowel type fasteners in the plane side of cross laminated timber and for edge joints were developed. Xu et al. [16] investigated the bearing capacity of single-bolted and multi-bolted glued timber-to-timber connections subjected to a load parallel to grain. The research showed that in all of the multi-row arrangements, the two-row cracks failure mode where the bolts were uniformly loaded exhibited the highest ductility. While ductile capacities calculated using the yield limit equations are quite reliable for fastener resistance in connections, however, they do not take into account the possible brittle failure mode of the connection which could be the governing failure mode in multi-fastener joints. Therefore, a stiffness-based design approach which has already been developed by Zarnani et al. [17] and verified in LVL (Laminated Veneer Lumber), glulam and lumber has been adapted to determine the block-tear out resistance of connections in CLT by considering the effect of perpendicular layers.

The researched CLT connections still have limited bearing capacity and have much room for improvement regarding seismic performance. The existing study about CLT is still in lack of the connection type which two rows of bolts are placed in both the wall panel and the floor panel in wall-to-floor connections and one bolt in each wall panel in wall-to-wall connections, and the failure modes of these types of connections are still uncertain. Furthermore, some known conclusions about common glued laminated timber bolted connections can not be fully applicable to CLT bolted connections. In addition, the bolted connections have advantages in terms of inexpensive cost, quickness in construction, high bearing capacity and reliable load transfer, hence the bolted connections have extensive application prospects. Thus in order to explore a kind of high-strength, earthquake-resistant, economical and suitable connection, 4 groups of CLT wall-to-floor and wall-to-wall bolted connections were tested in tension under monotonic and cyclic loading. The deformation characteristics and failure modes of the CLT wall-to-floor and wall-to-wall bolted connections were exploited. Load-slip curves, bearing capacity, yielding point, stiffness and ductility of each group of specimens were analyzed. A comparison of mechanic parameters and cost between CLT self-tapping screwed connections and bolted connections was performed, and some conclusions can be taken as reference.

2 Test Program

2.1 Design of Specimens

The experiment has 4 groups of CLT wall-to-floor and wall-to-wall bolted connections (in total 14 specimens). The CLT panels were manufactured by Ningbo Sino-Canada Low-Carbon Technology Research Institute. The raw materials for CLT panels were Canadian hemlock with no finger joints. Material properties for CLT panels are shown in Tab. 1. The total thickness of 3-layer CLT panels is 105 mm with each layer of 35 mm. Ruan et al. [18] also used this kind of wood material from the same company to conduct bending tests and rolling shear tests. The material property of metal angle brackets and steel bearing plates was Q235 in Chinese standard. The ordinary M12 bolts are of class 4.8. The labels of specimens and test configurations are shown in Tab. 2.

Table 1: Material properties for CLT panels

Density (kg/m³)	Moisture Content (%)	Elastic modulus parallel to grain (MPa)	Radial elastic modulus (MPa)	Chordwise elastic modulus (MPa)	Compression strength parallel to grain (MPa)	Compression strength perpendicular to grain (MPa)
443	13.7	14325	1177	333	31.0	10.4

Table 2: Test configurations and geometry

Conf. no.	Test configurations
A-MT-1 A-MT-2 A-CT-1 A-CT-2 A-CT-3	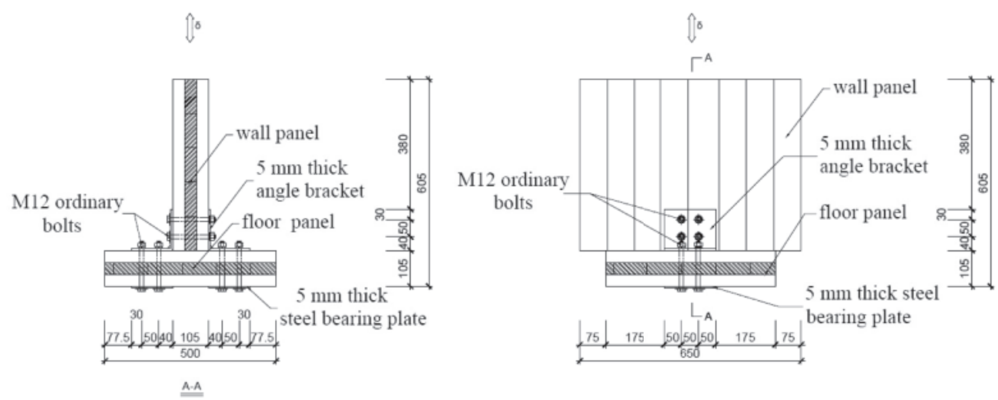
C-MT-1 C-MT-2 C-CT-1 C-CT-2 C-CT-3	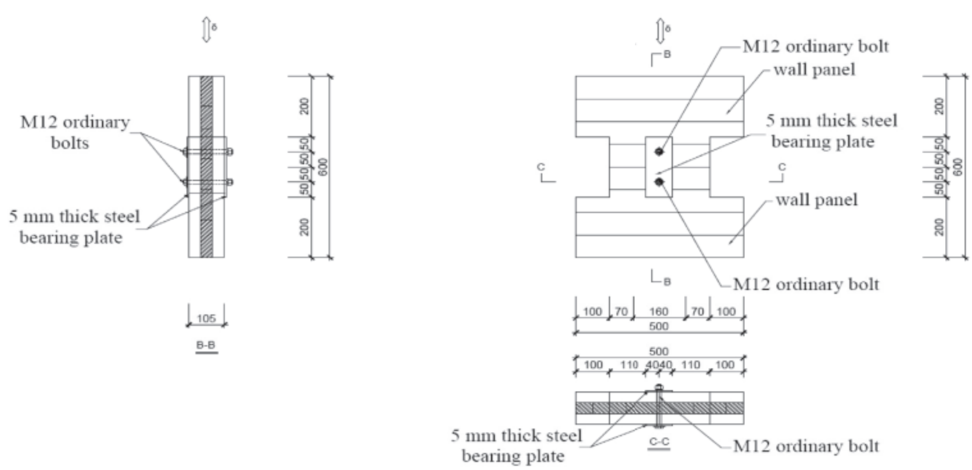

2.2 Test Setup and Measuring Contents

The loading apparatus and the layout of displacement testing points are shown in Fig. 1. The tensile monotonic loading and cyclic loading were performed by means of a hydraulic actuator POPWILL. The designed propulsive force of the actuator is ± 200 kN, and the displacement measurement range is

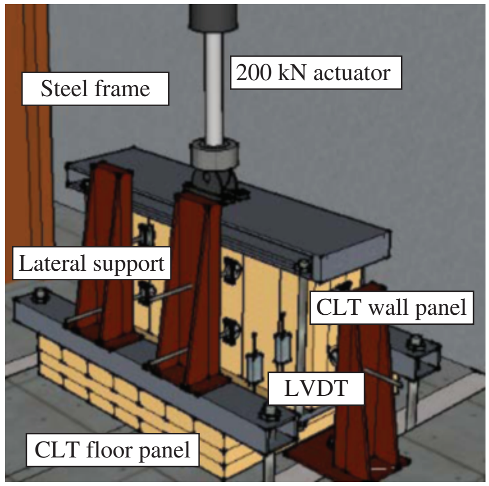

Figure 1: Test setup and instrumentation

± 500 mm. The main measuring parameters are as follows: (1) the force of the loading point directly outputted from the actuator; (2) the relative displacement of CLT wall-to-floor panels and wall-to-wall panels automatically recorded by the data collection software system. Furthermore, LVDT (Linear Variable Differential Transformer) were placed symmetrically alongside with CLT wall panels and floor panels to observe the possible torsion of specimens during the loading process.

2.3 Loading Protocol

Based on EN12512 [19], the monotonic loading was controlled at the slip rate of 0.05 mm/s, while the cyclic loading is 0.20 mm/s. The input yielding displacement for cyclic loading was obtained from the monotonic load-slip curve. The definition of yielding point can be visualized in Fig. 2. The cyclic loading protocol is shown in Fig. 3. For both monotonic and cyclic loading, the experiment should be stopped when unloaded to 80% of the maximum load.

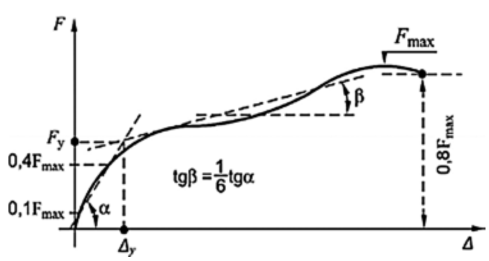

Figure 2: Definition of yielding point

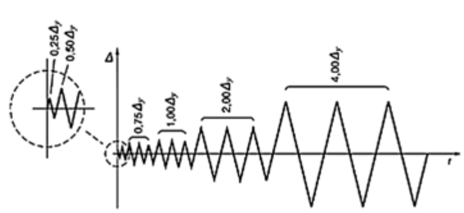

Figure 3: Procedure under cyclic loading

3 Experimental Results

3.1 Experimental Phenomenon

According to the deformation characteristics and the load-slip curves of specimens, five stages could be classified during the whole loading process.

1. **The elastic stage** (Fig. 6 segment oa). Neither obvious deformation nor any sound from the specimens could be noticed when loading. It could be represented by an ascending straight line in the load-slip curves.
2. **The slip stage** (Fig. 6 segment ab). The deformation of specimens could be visible in this stage. For group A, it could be observed that the wall panel moved upward gradually. A slight sound of "bang bang" could be heard due to the initial contact between bolts and the wall panel resulted from the slippage of bolts. For group C, the gap between two wall panels was remarkable.
3. **The embedding stage** (Fig. 6 segment bc). For group A, the movement of the wall panel was more significant when loading upward. At the same time, the sound of "bang bang" became low and urgent. It showed that the bolts and the wood had fully contacted with each other. The sound was caused by the compression perpendicular to grain in the outer layer of the wall panel and the compression parallel to grain in the inner layer of the wall panel. In the unloading stage, the deformation of the wall panel could be restored when small load was applied. However, unrecoverable residual deformation was caused when the load increased to a certain degree. For group C, the wall panel moved upward vertically when loaded, and the gap width between wall panels was up to 20 mm during the loading process. In the unloading stage, the upper wall panel rotated around the upper bolt continuously. Then the edge of the upper wall panel touched the lower wall panel. The upper wall panel moved downside until both the upper wall panel and the lower wall panel fitted together.
4. **The yielding stage** (Fig. 6 segment cd). For group A, slight deformation in the angle brackets appeared. The bolts also showed a sign of bending. At the same time, a very dense and crisp sound of "click" due to the wood splitting could be heard. The sound lasted for a long time and could serve as a clear warning signal. For group C, the bending of bolts was more obvious since there was only one bolt in the upper and lower wall panels respectively.
5. **The failure stage** (Fig. 6 segment de). The corresponding failure modes of each specimen of group A and group C are shown in Figs. 4 and 5 respectively. The corresponding failure modes of each specimen of group A is listed in Fig. 4, while the corresponding failure modes of each specimen of group C is shown in Fig. 5. For group A, the residual plastic deformation was distinct between the wall panel and the floor panel under monotonic tension (Fig. 4(c)). The connection failure occurred in the lower row of bolts in the side of angle bracket connected to the wall panel under monotonic tension (Fig. 4(b)), while the connection failure occurred in both the upper and lower rows of bolts in the side of angle bracket connected to the wall panel under cyclic loading (Fig. 4(f)). The bolts bent significantly at the failure stage, which indicated that the bolts had already yielded and formed plastic hinges. Compared with monotonic loading, the widening of bolt holes in the wall panel could be more observable during the cyclic loading (Fig. 4(f)). No matter in monotonic loading or cyclic loading, the bolts in the side of angle bracket remained almost intact. There was also recognizable plastic deformation in the angle brackets, which was an indication of the formation of plastic hinges in angle brackets. The failure mode was the splitting perpendicular to grain in the wall panel. For group C, the bolts bent heavily in both the monotonic and cyclic loading. The bolts yielded in the middle part along its length and formed single plastic hinge. Owing to the special build-up of CLT whose boards were stacked in orthogonality, the inner layer of the CLT panel was subjected to compression parallel to grain while the outer layer was in compression perpendicular to grain. The wood bearing capacity of compression parallel to grain was much higher than that of compression perpendicular to grain, which resulted in

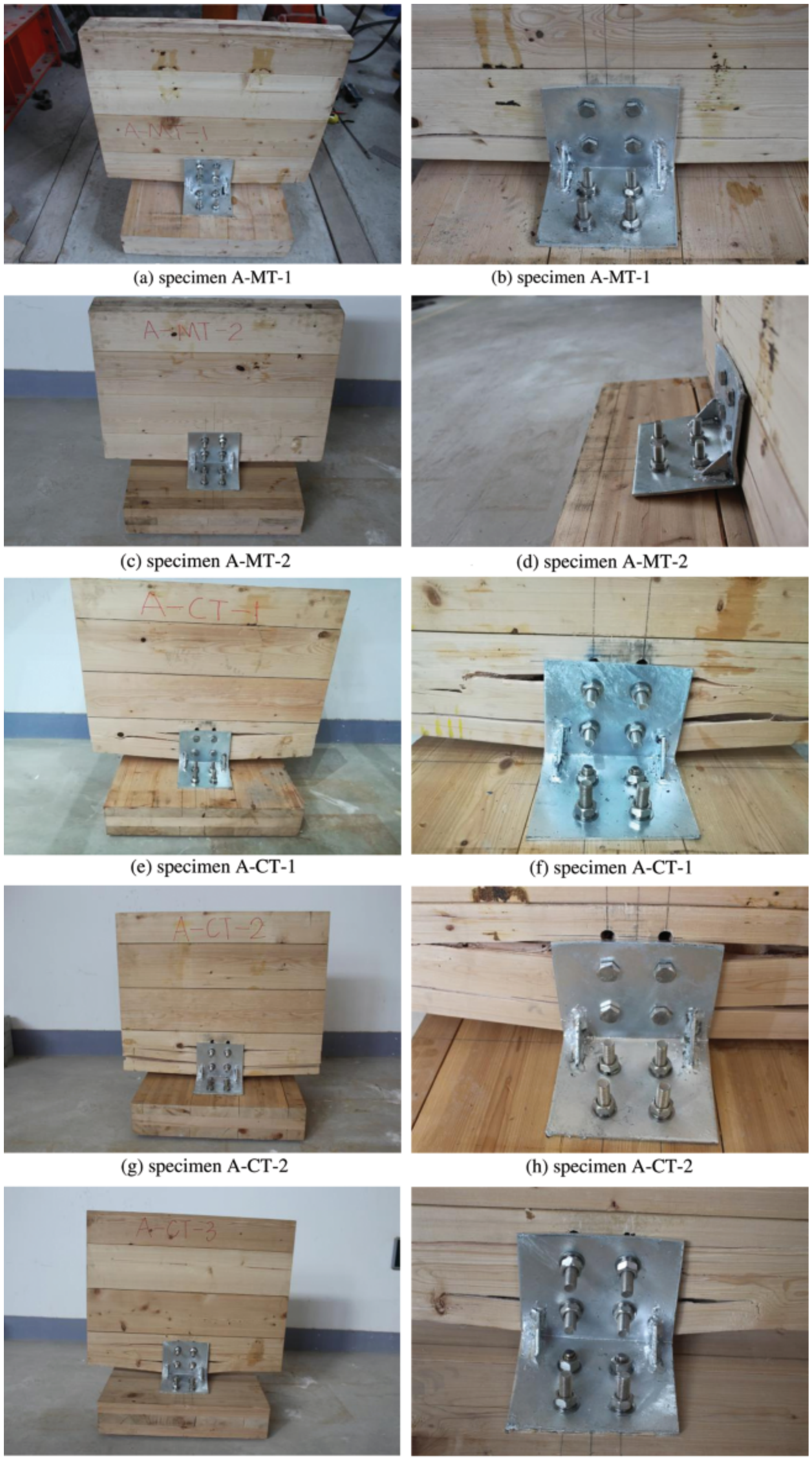

(a) specimen A-MT-1 (b) specimen A-MT-1

(c) specimen A-MT-2 (d) specimen A-MT-2

(e) specimen A-CT-1 (f) specimen A-CT-1

(g) specimen A-CT-2 (h) specimen A-CT-2

(i) specimen A-CT-3 (j) specimen A-CT-3

Figure 4: Typical failure modes of group A specimens: (b) the splitting of wood under compression perpendicular to grain in the lower row of bolts; (c) the residual plastic deformation between the wall panel and the floor panel; (f) the splitting of wood under compression perpendicular to grain in both the upper and the lower row of bolts

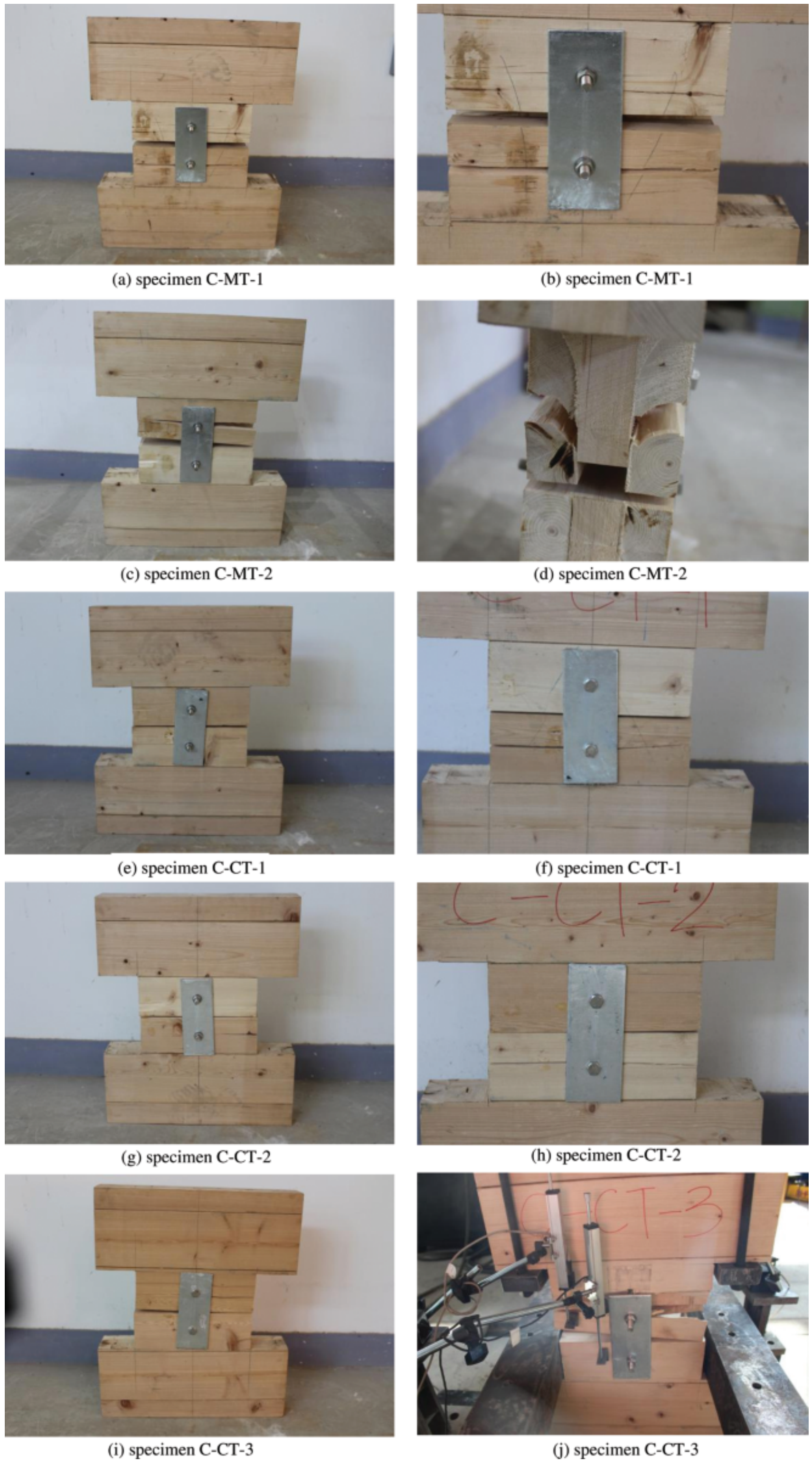

(a) specimen C-MT-1 (b) specimen C-MT-1

(c) specimen C-MT-2 (d) specimen C-MT-2

(e) specimen C-CT-1 (f) specimen C-CT-1

(g) specimen C-CT-2 (h) specimen C-CT-2

(i) specimen C-CT-3 (j) specimen C-CT-3

Figure 5: Typical failure modes of group C specimens: (a) the residual plastic deformation between wall panels; (b) the wood crack orientation of the upper and the lower wall panel; (d) the splitting failure perpendicular to grain in the outer layers of the wall panel

the yielding and the formation of single plastic hinge in bolts in the middle part along its length. There was also apparent residual plastic deformation between the wall panels after the connection failure (Fig. 5(a)). However, the steel bearing plate remained almost vertical during the loading process, and no obvious deformation could be seen in the steel bearing plate after the experiment. The failure mode is the splitting failure perpendicular to grain in the outer layers of CLT wall panel (Fig. 5(d)). The splitting failure perpendicular to grain in the wall panel occurred in both the upper wall panel and the lower wall panel connected with the steel bearing plate (Fig. 5(b)).

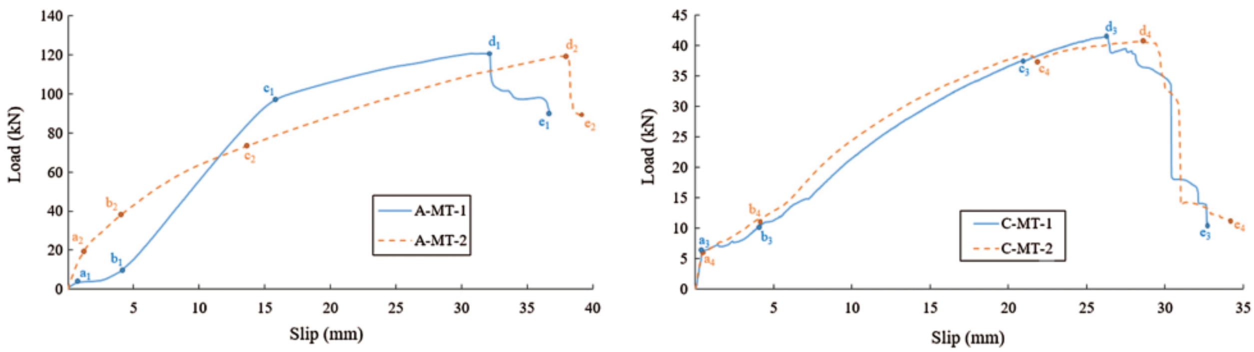

(a) group A (b) group C

Figure 6: Monotonic load-slip curves of specimens: (a) wall-to-floor bolted connections under monotonic loading; (b) wall-to-wall bolted connections under monotonic loading

3.2 Load-Slip Curves

The monotonic load-slip curves for specimens are shown in Fig. 6. The load corresponds to the force exerted by the actuator and the slip represents vertical displacement of the actuator.

For group A monotonic loading (Fig. 6(a)), there was an initial low stiffness range in the load-slip curve for specimen A-MT-1 within the slip of 3 mm because of the gap between bolts and the specimen, but that was not the case for specimen A-MT-2. Although the load-slip curves for specimen A-MT-1 and A-MT-2 deviate from each other, the ultimate load of these two specimens is quite similar, and there is no significant difference between their ultimate displacement too. It is evident to distinguish the elastic stage from the plastic stage from the their load-slip curves.

For group C monotonic loading (Fig. 6(b)), the load-slip curves of specimen C-MT-1 and specimen C-MT-2 are in good agreement. The loading paths of the two specimens are almost identical. It’s obvious to differentiate the elastic stage, the slip stage, the embedding stage, the yielding stage and the failure stage.

Seen from the load-slip curves of group A and group C, it’s not hard to note that the plastic performance of group A is better than group C. The envelope area under load-slip curve of group A is larger than that of group C, which indicates that the energy dissipation ability of group A is greater than that of group C, namely group A is better than group C in ductility. The reason behind this lies in that there were four bolts to dissipate energy in the wall panel in group A while there were only two bolts in the wall panels in group C.

The hysteresis curves for specimens are shown in Fig. 7. The load corresponds to the force exerted by the actuator and the slip is the vertical displacement of the actuator.

At the initial loading stage, the specimens were in linear elastic state, which could be represented by an ascending straight line in the load-slip curves. At this stage, the loading and unloading curves generally coincided with no residual strain. With the constant increase of loading, the bolts began to slip, indicated by the decrease of the curve slope. At the same time, the residual strain accumulated and the hysteretic

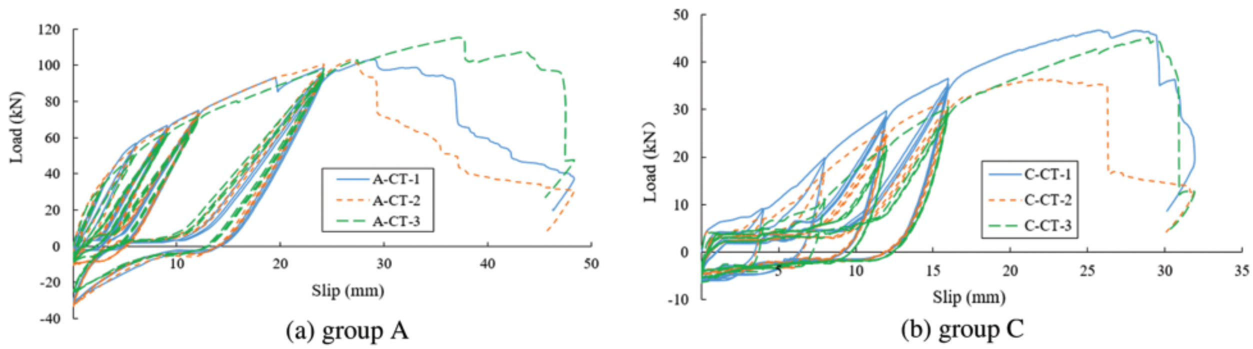

Figure 7: Hysteresis curves of specimens: (a) wall-to-floor bolted connections under cyclic loading; (b) wall-to-wall bolted connections under cyclic loading

loop area gradually increased. Subsequently, the specimens entered the embedding stage with increment of load and decline of stiffness. After that the bolts in the specimens yielded, and the load rise was not apparent, which could be demonstrated by the stagnant trend in the load-slip curve. Ultimately, the connection suffered from a plunge failure, seen from the load-slip curve. Before reaching the ultimate limit state, the load of the specimens was continuously strengthened, while the stiffness degraded constantly in the whole process of the loading. There had been quite large plastic deformation before connection failure, which could serve as a clear warning signal.

From the hysteresis curves of group A and group C, the hysteretic loop of group A is plumper than that of group C, which indicates that the specimens of group A have a stronger ability to dissipate energy.

4 Study of Mechanical Parameters

4.1 Mechanical Parameters

Mechanical parameters of the CLT bolted connections can be obtained from the load-slip curves. The mechanical parameters are defined as follows.

1. maximum load F_{max} and maximum displacement Δ_{max}
   F_{max} corresponds to the maximum load reached during the experiment, and Δ_{max} is defined as the slip corresponding to the maximum load F_{max}.
2. ultimate load F_u and ultimate displacement Δ_u
   F_u is taken as 80% of the maximum load F_{max}, namely F_u = 0.8 F_{max}, and Δ_u is defined as the slip corresponding to the ultimate load F_u.
3. yielding load F_y and yielding displacement Δ_y
   According to the definition of yielding point prescribed by EN12512 [19], a straight line l_1 is drawn connecting two points of 0.1 F_{max} and 0.4 F_{max}, and the angle of slope of line l_1 is termed as α. Then a point Q is found from the load-slip curve whose tangential angle of slope β satisfies $\text{tg}\beta = \frac{1}{6}\text{tg}\alpha$. Mark this tangent line as l_2, and the intersection point of line l_1 and line l_2 is the yielding point. The load corresponds to the yielding point is the yielding load F_y, and the corresponding slip is the yielding displacement Δ_y (shown as Fig. 2).
4. initial stiffness K_{ser}
   K_{ser} is taken as the slope between two points of of $0.1F_{max}$ and $0.4F_{max}$, namely $K_{ser} = \frac{0.4F_{max} - 0.1F_{max}}{\Delta_{0.4F_{max}} - \Delta_{0.1F_{max}}}$.
5. ductility ratio D
   D is measured by the ratio between ultimate displacement Δ_u and yielding displacement Δ_y, namely $D = \frac{\Delta_u}{\Delta_y}$.

4.2 Analysis of Mechanical Parameters

For monotonic and cyclic loading, mechanic parameters of specimens are shown in Tab. 3. The ultimate loads for group A are of 82.42-96.55 kN, with the mean value of 89.85 kN. The ultimate loads for group C are of 29.10-37.34 kN, with the mean value of 33.65 kN. The average ultimate load for group A is 2.67 times that of group C. The average initial stiffness for group A is 8.69 kN/mm, while the average initial stiffness for group C is 1.75 kN/mm. The average initial stiffness for group A is approximately 5 times that of group C. The average ductility ratio for group A is 4.38, and the average ductility ratio for group C is 1.58, indicating that the ductility of group A is better than group C. However, it should be pointed out that the yielding displacement variation coefficient for group A is 42%, while the yielding displacement variation coefficient for group C is only 15%. The ductility ratio correlates with the yielding displacement, which indirectly means that the representative of the ductility ratio for group A is weaker than that for group C.

Table 3: Mechanic parameters of specimens

Conf. No.	F_{max} (kN)	Δ_{max} (mm)	F_u (kN)	Δ_u (mm)	K_{ser} (kN/mm)	F_y (kN)	Δ_y (mm)	D (−)
A-MT-1	120.69	30.84	96.55	36.41	7.83	98.58	15.54	2.34
A-MT-2	119.34	37.52	95.47	38.47	6.72	88.92	12.08	3.19
A-CT-1	103.14	28.96	82.51	36.90	10.72	62.09	5.65	6.53
A-CT-2	103.02	26.76	82.42	29.28	10.12	70.42	6.44	4.55
A-CT-3	115.40	37.26	92.32	47.26	8.06	77.86	8.90	5.31
C-MT-1	41.53	26.34	33.22	30.38	1.64	40.24	22.34	1.36
C-MT-2	40.69	28.54	32.55	30.22	1.93	33.41	15.47	1.95
C-CT-1	46.68	25.65	37.34	30.65	1.94	36.83	17.00	1.80
C-CT-2	36.37	22.07	29.10	26.16	1.53	36.10	21.34	1.23
C-CT-3	45.04	28.95	36.03	30.87	1.71	34.13	19.71	1.57

The experimental results of CLT bolted connections are compared with the experimental results of CLT self-tapping screwed connections from Xiong et al. [20]. The values listed in Tab. 4 are the mean value of the respective monotonic and cyclic mechanical parameters. For CLT wall-to-floor connections, the ultimate load for bolted connections is 2.70 times that for self-tapping screwed connections. The ultimate displacement for bolted connections is 75% that for self-tapping screwed connections. The yielding load for bolted connections is 4.08 times that for self-tapping screwed connections. The yielding displacement for bolted connections is 2.26 times that for self-tapping screwed connections. The ductility ratio correlates with the yielding displacement, which leads to the ductility ratio for bolted connections is only 36% that for self-tapping screwed connections. For CLT wall-to-wall connections, the ultimate load for bolted connections is 3.83 times that for self-tapping screwed connections. The ultimate displacement is 4.95 times that for self-tapping screwed connections. The yielding load for bolted connections is 3.90 times that for self-tapping screws. The yielding displacement for bolted connections is 11.02 times that for self-tapping screwed connections. The yielding displacement of bolted connections is much larger than that that of self-tapping screwed connections, which leads to a 55% ductility ratio reduction in bolted connections than in self-tapping screwed connections. Analyzed from Tab. 3, Figs. 6 and 7 and compared with self-tapping screwed connections from Tab. 4, bolted connections have a higher bearing capacity, larger yielding displacement, a wider plastic range, stronger ability to dissipate energy, better ductility, and a more clear warning signal before failure.

Table 4: Comparison of average mechanic parameters of specimens between CLT bolted connections and self-tapping screwed connections

Parameter	Group A self-tapping screwed connections	Group A bolted connection	Parameter value ratio of group A bolted connections to self-tapping connections	Group C self-tapping screwed connections	Group C bolted connections	Parameter value ratio of group C bolted connections to self-tapping connections
F_{max} (kN)	41.61	112.32	2.70	10.98	42.06	3.83
Δ_{max} (mm)	40.33	32.27	0.80	3.93	26.31	6.69
F_u (kN)	33.31	89.85	2.70	8.78	33.65	3.83
Δ_u (mm)	50.53	37.66	0.75	5.99	29.66	4.95
K_{ser} (kN/mm)	4.52	8.69	1.92	5.34	1.75	0.33
F_y (kN)	19.51	79.57	4.08	9.27	36.14	3.90
Δ_y (mm)	4.30	9.72	2.26	1.74	19.17	11.02
D (−)	12.26	4.38	0.36	3.53	1.58	0.45

5 Comparison of Expenditure

The cost of CLT single bolted connection in this paper is compared with the cost of CLT single self-tapping screwed connection from Xiong et al. [20]. The comparison results are listed in Tab. 5, and all fees include prime cost, added-value tax, freight, import agent fee and customs duties. When comparing the cost of group C, the cost of the two steel bearing plates in CLT bolted connections is not included because there were no steel bearing plates in self-tapping screwed connections. For CLT wall-to-floor connections, the cost of bolted connections is 46% that of self-tapping screwed connections. For CLT wall-to-wall connections, the cost of bolted connections is 53% of self-tapping screwed connections. In general, bolted connections are more competitive than self-tapping screwed connections in terms of cost.

Table 5: Comparison of expenditure between cross-laminated timber bolted connections and self-screwed connections

Cost	Group A self-tapping screwed connections	Group A bolted connections	Cost ratio of group A bolted connections to self-tapping screwed connections	Group C self-tapping screwed connections	Group C bolted connections	Cost ratio of group C bolted connections to self-tapping screwed connections
Amount (RMB)	190.0	88.3	0.46	14.4	7.7	0.53

6 Conclusions

This paper presents the study of cross-laminated timber wall-to-floor and wall-to-wall bolted connections under monotonic tension and cyclic loading. The deformation characteristics and failure modes of the cross-laminated timber wall-to-floor and wall-to-wall bolted connections were exploited. Load-slip curves, bearing capacity, yielding point, stiffness and ductility of each group of specimens were analyzed. A comparison of mechanic parameters and cost between cross-laminated self-tapping screwed connections and bolted connections was performed, and conclusions can be drawn as follows.

1. The loading process of cross-laminated timber bolted connections under tension can be categorized as five stages, namely the elastic stage, the slip stage, the embedding stage, the yielding stage and the ultimate stage.
2. For cross-laminated timber wall-to-floor connections, the failure mode is the splitting of the wall panel perpendicular to grain. The connection failure occurred in the lower row of bolts in the side of angle bracket connected to the wall panel under monotonic tension, while the connection failure occurred in both the upper and lower rows of bolts in the side of angle bracket connected to the wall panel under cyclic loading. For cross-laminated timber wall-to-wall connections, the failure mode is the splitting failure perpendicular to grain in the outer layers of the wall panel. The splitting failure perpendicular to grain in the wall panel occurred in both the upper wall panel and the lower wall panel connected with the steel bearing plate.
3. The ultimate tensile bearing capacity for cross-laminated timber wall-to-floor bolted connections is stronger than that for wall-to-wall bolted connections. The hysteretic loop of cross-laminated timber wall-to-floor connections is plumper than that of wall-to-wall connections, and the specimens of cross-laminated timber wall-to-floor connections have a stronger ability to dissipate energy than that of wall-to-wall connections.
4. Compared with cross-laminated timber self-tapping screwed connections, bolted connections have a higher bearing capacity, larger yielding displacement, a wider plastic range, stronger ability to dissipate energy, better ductility, and a more clear warning signal before failure.
5. Cross-laminated timber bolted connections are more competitive than self-tapping screwed connections in terms of cost.

Acknowledgement: The authors would like to acknowledge with much appreciation the support from Dr. Brad Jianhe Wang (Adjunct Professor of University of New Brunswick) and Ningbo Sino-Canada Low Carbon Technology Research Institute.

Funding Statement: This study is funded by the Fundamental Research Funds for the Central Universities (Program No. 22120180315).

Conflicts of Interest: The authors declare that they have no conflicts of interest to report regarding the present study.

References

1. Mahdavifar, V., Barbosa, A. R., Sinha, A., Muszynski, L., Gupta, R. (2016). Hysteretic behaviour of metal connectors for hybrid (high- and low-grade mixed species) cross laminated timber. *14th World Conference on Timber Engineering, 22-25 August, Vienna, Austria*.
2. Muñoz, W., Mohammad, M., Gagnon, S. (2010). Lateral and withdrawal resistance of typical CLT connections. *Proceedings of the 11th World Conference on Timber Engineering, 20-24 June, Riva del Garda, Italy.*
3. Flatscher, G., Bratulic, K., Schickhofer, G. (2014). Screwed joints in cross laminated timber structures. *13th World Conference on Timber Engineering, 10-14 August, Quebec, Canada*.
4. Gavric, I., Fragiacomo, M., Ceccotti, A. (2015). Cyclic behavior of typical screwed connections for cross-laminated (CLT) structures. *European Journal of Wood and Wood Products, 73(2),* 179–191. DOI 10.1007/s00107-014-0877-6.
5. Gavric, I., Fragiacomo, M., Ceccotti, A. (2014). Cyclic behavior of typical metal connectors for cross-laminated (CLT) structures. *Materials and Structures, 48(6),* 1841–1857. DOI 10.1617/s11527-014-0278-7.

6. Tomasi, R. (2013). Seismic behavior of connections for buildings in CLT. *Focus Solid Timber Solution - European Conference on Cross Laminated Timber (CLT), Theme III,* 138–151.
7. Izzi, M., Flatscher, G., Fragiacomo, M., Schickhofer, G. (2016). Experimental investigations and design provisions of steel-to-timber joints with annular-ringed shank nails for Cross-Laminated Timber structures. *Construction and Building Materials, 122,* 446–457. DOI 10.1016/j.conbuildmat.2016.06.072.
8. Shen, Y. L., Schneider, J., Tesfamariam, S., Stiemer, S. F., Mu, Z. G. (2013). Hysteresis behavior of bracket connection in cross-laminated-timber shear walls. *Construction and Building Materials, 48,* 980–991. DOI 10.1016/j.conbuildmat.2013.07.050.
9. Cao, J. X., Xiong, H. B., Chen, J. W., Huynh, A. (2019). Bayesian parameter identification for empirical model of CLT connections. *Construction and Building Materials, 218,* 254–269. DOI 10.1016/j.conbuildmat.2019.05.051.
10. Latour, M., Rizzano, G. (2017). Seismic behavior of cross-laminated timber panel buildings equipped with traditional and innovative connectors. *Archives of Civil & Mechanical Engineering, 17(2),* 382–399. DOI 10.1016/j.acme.2016.11.008.
11. European Organisation for Technical Assessment (EOTA) (2015). Rotho Blaas X-RAD, European Technical Approval ETA-15/0632, Vienna, Austria.
12. Bejtka, I., Blaß, H. J. (2002). Joints with inclined screws. *Proceeding of the Meeting 35 of the Working Commission W18-Timber Structures, CIB,* Vancouver, Canada.
13. Ringhofer, A., Brandner, R., Schickhofer, G. (2015). Withdrawl resistance of self-tapping screws in unidirectional and orthogonal layered timber products. *Materials and Structures, 48(5),* 1435–1447. DOI 10.1617/s11527-013-0244-9.
14. Ringhofer, A., Brandner, R., Blaß, H. J. (2018). Cross laminated timber (CLT): design approaches for dowel-type fasteners and connections. *Engineering Structures, 171,* 849–861. DOI 10.1016/j.engstruct.2018.05.032.
15. Uibel, T., Blaß, H. J. (2013). Joints with dowel type fasteners in CLT structures. In: Harris, R., Ringhofer, A., Schickhofer, G., (eds.) *COST Action FP1004: Focus Solid Timber Solutions–European Conference On Cross Laminated Timber (CLT)*. Bath: The University of Bath.
16. Xu, D. L., Liu, W. Q., Zhou, D., Xi, A. F. (2011). Experimental study of bolted glued timber-to-timber joints. *Journal of Building Structures, 32(7),* 93–100.
17. Zarnani, P., Quenneville, P. (2015). New design approach for controlling brittle failure modes of small-dowel-type connections in Cross-laminated Timber (CLT). *Construction and Building Materials, 100,* 172–182. DOI 10.1016/j.conbuildmat.2015.09.049.
18. Ruan, G. M., Xiong, H. B., Chen, J. W. (2019). Bending and rolling shear properties of cross-laminated timber fabricated with Canadian hemlock. *Structural Durability and Health Monitoring, 13(2),* 227–246. DOI 10.32604/sdhm.2019.04743.
19. EN12512:2001. *Timber structures-test methods-cyclic testing of joints made with mechanical fasteners*. Brussels: European Committee for Standardisation.
20. Xiong, H. B., Huynh, A. (2018). Mechanical behaviour of connections between CLT panels under monotonic and cyclic loading. *2nd International Workshop on Renewable Energy and Development IOP Conference Series: Earth and Environmental Science, 20-22 April, Guilin, China*.